European Journal of Pharmacology 945 (2023) 175613

Contents lists available at ScienceDirect

European Journal of Pharmacology

journal homepage: www.elsevier.com/locate/ejphar

Probing the effects of MR120 in preclinical chronic colitis: A first-in-class anti-IBD agent targeting the CCL20/CCR6 axis

Marika Allodi [a], Carmine Giorgio [a], Matteo Incerti [a], Domenico Corradi [b], Lisa Flammini [a], Vigilio Ballabeni [a], Elisabetta Barocelli [a], Marco Radi [a,*], Simona Bertoni [a,**]

[a] Dipartimento di Scienze degli Alimenti e del Farmaco, Università degli Studi di Parma, Viale Delle Scienze, 27/A, 43124, Parma, Italy
[b] Dipartimento di Medicina e Chirurgia, Università degli Studi di Parma, Via Gramsci 14, 43126, Parma, Italy

ARTICLE INFO

Keywords:
DSS-Induced chronic colitis
CCR6 antagonist
Intestinal inflammation

ABSTRACT

Concerning the growing interest in the role played by the CCL20/CCR6 axis in IBD pathogenesis and in the search for novel anti-IBD small molecules, we have recently discovered the first small-molecule (MR120) endowed with protective action against TNBS-induced colitis and zymosan-induced peritonitis. This protective action occurs through interference with the CCL20/CCR6 signaling. The aim of the present work is to expand the preclinical investigation of MR120, evaluating its beneficial anti-inflammatory effect on a model of chronic colitis obtained by cyclically exposing C57BL/6 mice to 3% DSS. Subcutaneous administration of MR120 at 1 mg/kg, the same dose effective against acute inflammation, helped attenuate several systemic and local inflammatory responses induced by DSS. Besides significantly improving murine health conditions, MR120 counteracted mucosal macroscopic injury, the increase of colonic edema and neutrophils oxidative activity, and mitigated spleen enlargement, while not significantly lowering intestinal IL-6 concentration. Overall, repeated daily treatment with MR120 for approximately 30 days was well tolerated and showed moderate protection in a relevant model of chronic colitis, in line with the beneficial effect previously observed in acute models of intestinal inflammation. Although more potent analogues of MR120 will be needed to more fully evaluate their clinical translatability, the present work provides a valuable example of *in vivo* efficacy of CCL20/CCR6 modulators in a chronic model of IBD.

1. Introduction

Chemokine receptor 6 (CCR6) and its sole ligand, the chemokine ligand 20 (CCL20), form an exclusive ligand-receptor pair that has emerged as a potentially exploitable target in the search for novel small molecule drug candidates for inflammatory bowel disease (IBD) (Trivedi and Adams, 2018; Meitei et al., 2021). CCR6 is mainly expressed by immune cells, such as $CD4^+$ and $CD8^+$ T lymphocytes, B cells, antigen-presenting cells, activated neutrophils, and is known to drive their migration to the intestine in response to CCL20 released by immune and non-immune elements of the inflamed area (Lee et al., 2013). A number of clinical and preclinical observations support the participation of the CCL20/CCR6 axis in the pathogenesis of IBD, a complex of chronic relapsing inflammatory disorders of the intestine, where anomalous immune responses exert a key role. Firstly, the increased mucosal and plasmatic expression of these chemokines was evidenced both in human IBD (Kaser et al., 2004; Skovdahl et al., 2015, 2018) and in murine models of Th1-dependent colitis, in IL10−/− mice and in chronic adoptive transfer colitis (Scheerens et al., 2001). Secondly, distinct strategies interfering with this pathway, either CCR6-knockout mice (Varona et al., 2003) or administration of anti-CCL20 neutralizing antibodies (Katchar et al., 2007; Teramoto et al., 2005), were effective in preventing colonic injury. However, up to now the pharmacological blockade of the CCL20/CCR6 axis for the treatment of IBD has been attempted in preclinical studies only with biological agents, none of which have been clinically approved yet.

Recently, by applying a mechanistic-informed phenotypic drug discovery approach, we have discovered a small-molecule that represents a first-in-class inhibitor for IBD by targeting the CCL20/CCR6 axis: the 3-methyl-N-(4-(trifuoromethyl)phenyl)benzofuran-2-carboxamide (MR120; Fig. 1). Starting from multicomponent reactions (MCR) previously set up in our group (Vincetti et al., 2016), a large virtual

* Corresponding author.
** Corresponding author.
E-mail addresses: marco.radi@unipr.it (M. Radi), simona.bertoni@unipr.it (S. Bertoni).

https://doi.org/10.1016/j.ejphar.2023.175613
Received 5 January 2023; Received in revised form 17 February 2023; Accepted 20 February 2023
Available online 24 February 2023

combinatorial library of synthetically accessible derivatives was designed and virtually screened on a CCR6 homology model. The top ranking compounds were synthesized using the original MCR protocols and were submitted to a sequence of functional and targeted assays. MR120 was identified as the most promising compound to disrupt the CCL20-induced chemotaxis of $CCR6^{+}CD4^{+}$ T cells by acting as antagonist of the CCR6 receptor and interfering with both β-arrestin and miniGi recruitment. *In vivo* MR120 mitigated the inflammatory responses both in TNBS-induced colitis, an acute model of intestinal inflammation characterized by the activation of Th1-dependent adaptive immunity, and in zymosan-induced peritonitis, a model of phlogistic response associated with strong leukocytes recruitment. Specifically, MR120 improved the overall conditions of mice, attenuated colonic macroscopic injury and counteracted local and systemic neutrophils oxidative activity, mitigating leukocytes responses in acute peritoneal inflammation as well (Martina et al., 2022).

In order to better elucidate the potential anti-IBD properties of MR120 and to provide further information on the participation of the CCL20/CCR6 pathway in the development of intestinal inflammation, the present work has focused on the evaluation of the protective anti-inflammatory effect of MR120 in a mouse model of dextran sulfate sodium (DSS)-induced chronic colitis. Indeed, among the different preclinical models of colitis, murine DSS-induced chronic colitis stands out as a model of long-term disease characterized by recurrent exacerbations and remissions, mimicking the typical progression of human IBD, and marked by the involvement of mixed Th1 and Th2 responses (Alex et al., 2009).

Notably, a relevant property of the DSS model is its predictive validity, providing recognition of novel candidate molecules as potential anti-IBD drugs with clinical efficacy (Axelsson et al., 1998; Valatas et al., 2015). Accordingly, the local and systemic effects of MR120 1 mg/kg have been herein investigated after parenteral administration in a murine model of chronic colitis, induced by three-cycle drinking of DSS, and compared to the responses exhibited in vehicle-treated colitic mice.

2. Materials and methods

2.1. Animals

All animal experiments were performed according to the guidelines for the use and care of laboratory animals and they were authorized by the local Animal Care Committee "Organismo Preposto al Benessere degli Animali" and by Italian Ministry of Health, "Ministero della Salute" (Protocol Number 38/2017-PR). All appropriate measures were taken to minimize pain or discomfort of animals. C57BL/6 mice (7–12 weeks old) (Charles River Laboratories, Calco, Italy), weighing 20–25g, were housed five per cage and maintained under standard conditions at our animal facility (12:12 h light–dark cycle, water and food *ad libitum*, 22–24 °C). All the experimental procedures and euthanasia by CO_2 inhalation were performed between 9 a.m. and 2 p.m.

2.2. Induction of colitis

C57BL/6 mice were exposed to 3% (w/v) dextran sulfate sodium (DSS, MW: 36–50 kDa, purchased from Cayman Chemical, MI 48108, USA) dissolved in autoclaved tap water and administered *ad libitum* for 3

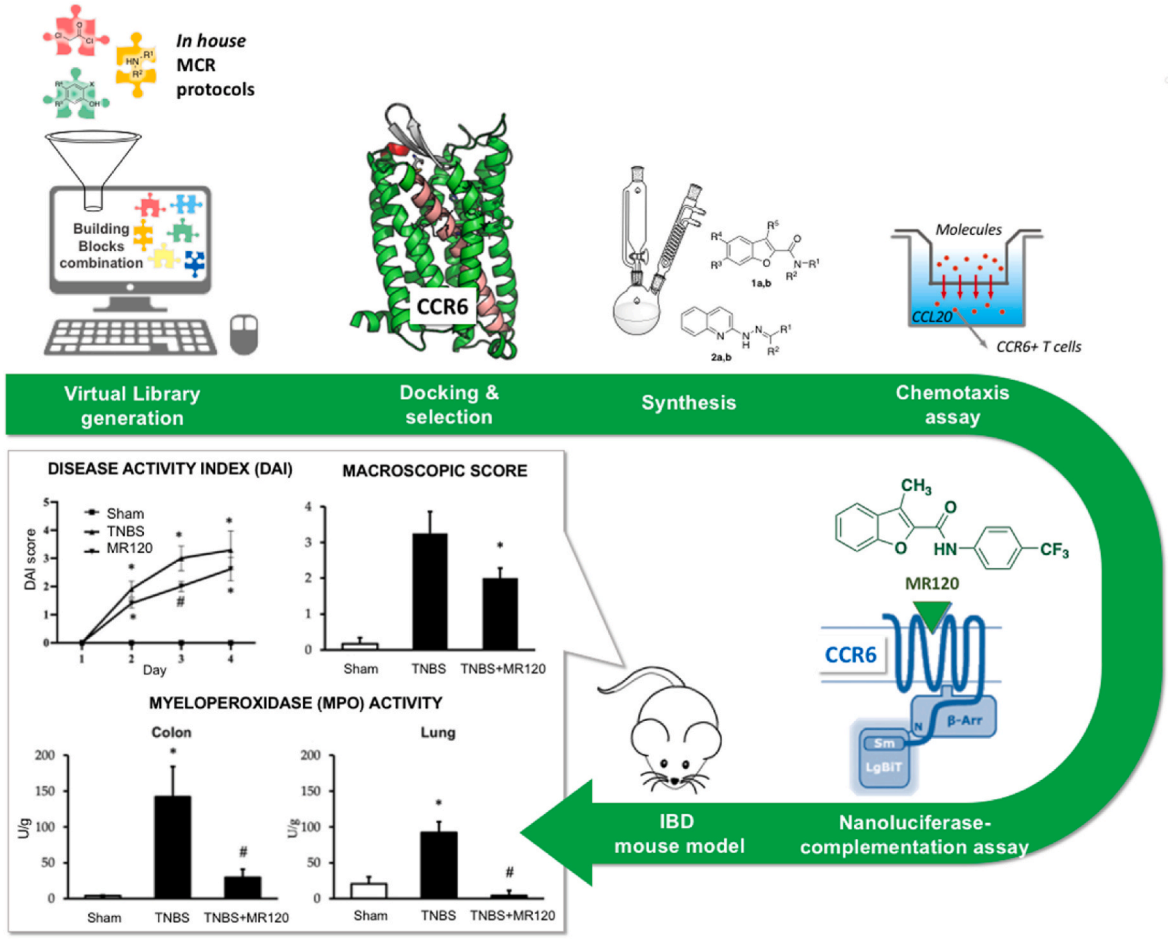

Fig. 1. Mechanistic-informed phenotypic drug discovery approach for the discovery of MR120 and *in vivo* data on the TNBS model (adapted from Martina et al., 2022).

cycles (5 days of DSS), interspersed with 9 days of tap water only. From day 8 onwards until day 32, mice were subcutaneously (s.c.) treated with MR120 or with vehicle, twice daily (b.i.d.) and 8 h apart, by a researcher not involved in the daily monitoring of disease activity index (DAI) or in biochemical or histological assays.

At the end of the third cycle of exposure to DSS (day 33), mice were euthanized by CO_2 inhalation according to the scheme represented in Table 1.

2.3. Experimental design

Mice were assigned through block randomization to the following experimental groups.

- sham group (S) (n = 9), receiving drinking water and s.c. administered with vehicle (DMSO 1% in saline solution; 10 ml/kg);
- control group (C) (n = 9), receiving DSS 3% in drinking water and s.c. administered with vehicle (DMSO 1% in saline solution; 10 ml/kg);
- MR120 group (MR) (n = 11), receiving DSS 3% in drinking water and s.c. administered with MR120 1 mg/kg.

The dosage of MR120 was chosen on the basis of (Martina et al., 2022). The study was performed using experimental blocks composed of 9 mice that were randomly assigned to S, C and MR groups of treatments, each one encompassing 3 animals.

2.4. Evaluation of inflammatory responses

Body weight, stools consistency and rectal bleeding were examined and registered daily throughout the experimentation by unaware observers, in order to assess the Disease Activity Index (DAI). Immediately after euthanasia, the macroscopic damage of colonic mucosa was assessed as macroscopic score (MS) after visual inspection. Colon, lungs, spleen and mesenteric lymph nodes were collected for subsequent microscopic, biochemical or flow cytometry analyses.

2.4.1. Disease activity index (DAI)

DAI is a parameter that estimates the severity of the disease; it consists of the daily assignment of a total score, according to Cooper's modified method (Cooper et al., 1993), on the basis of body weight loss, stool consistency and rectal bleeding. The scores were attributed blindly and were quantified as follows (max = 6): stool consistency: 0 (normal), 1 (soft), 2 (liquid); body weight loss: 0 (<5%), 1 (5–10%), 2 (10–15%), 3 (15–20%), 4 (20–25%), 5 (>25%); rectal bleeding: 0 (absent), 1 (present).

2.4.2. Colon macroscopic damage score (MS)

After euthanasia, the colon was explanted, opened longitudinally, flushed with saline solution and MS was immediately evaluated through inspection of the mucosa, executed by two investigators unaware of the treatments applied. MS was determined according to previously published criteria (Giorgio et al., 2021), as the sum of scores (max = 14) attributed as follows: presence of strictures and hypertrophic zones (0, absent; 1, 1 stricture; 2, 2 strictures; 3, more than 2 strictures); mucus (0, absent; 1, present); adhesion areas between the colon and other intra-abdominal organs (0, absent; 1, 1 adhesion area; 2, 2 adhesion areas; 3, more than 2 adhesion areas); intraluminal hemorrhage (0, absent; 1, present); erythema (0, absent; 1, presence of a crimsoned area <1 cm^2; 2, presence of a crimsoned area >1 cm^2); ulcerations and necrotic areas (0, absent; 1, presence of a necrotic area <0.5 cm^2; 2, presence of a necrotic area ≥0.5 cm^2 and <1 cm^2; 3, presence of a necrotic area ≥1 cm^2 and <1.5 cm^2; 4, presence of a necrotic area ≥1.5 cm^2).

2.4.3. Colonic length, thickness and edema

The length of the colon and its wet weight were measured to assess deposition of fibrotic material and muscular contraction elicited by colitis induction: weight/length ratio was calculated to assess colon thickness, according to previously published criteria (Grandi et al., 2017).

The increased capillary permeability of colonic mucosa, expressed as increased tissue water content, was determined using the wet-to-dry weight ratio according to (Moore-Olufemi et al., 2005). Colonic samples about 0.5 cm in length were excised from each mouse, cut along the anti-mesenteric border and weighed (wet weight). Tissues were dried over 72 h and dry weights were measured. Tissue water content was determined and expressed as ratio (wet weight - dry weight)/dry weight.

2.4.4. Colonic and pulmonary myeloperoxidase (MPO) activity assay

MPO activity, marker of tissue granulocytic infiltration, was determined according to Ivey's modified method (Ivey et al., 1995) in colon and lungs. After being weighed, each colonic or lung sample was homogenized in ice-cold 0.02 M sodium phosphate buffer (pH 4.7), containing 0.015 M Na_2EDTA and 1% Halt Protease Inhibitor Cocktail (ThermoFisher Scientific), and centrifuged for 20 min at 12500 RCF at 4 °C. Pellets were re-homogenized in 4 vol of ice-cold 0.2 M sodium phosphate buffer (pH 5.4) containing 0.5% hexadecylthrimethyl-ammoniumbromide (HTAB) and 1% Halt Protease Inhibitor Cocktail (ThermoFisher Scientific). Samples were then subjected to 3 cycles of freezing and thawing and centrifuged for 30 min at 15500 RCF at 4 °C. 50 μL of the supernatant was then allowed to react with 950 μL of 0.2 M sodium phosphate buffer, containing 1.6 mM tetramethylbenzidine, 0.3 mM H_2O_2, 12% dimethyl formamide, 40% Dulbecco's phosphate buffered saline (PBS). Each assay was performed in duplicate and the rate of change in absorbance was measured spectrophotometrically at 690 nm (TECAN Sunrise™ powered by Magellan™ data analysis software, Mannedorf, Switzerland). 1 unit of MPO was defined as the quantity of enzyme degrading 1 μmol of peroxide per minute at 25 °C. Data were normalized with edema values and expressed

Table 1
Experimental scheme for DSS chronic colitis and pharmacological treatments.

	Day 1-5	Day 6-14	Day 15-19	Day 20-28	Day 29-33
Sham	Water	Water	Water	Water	Water
Control	3% DSS	Water	3% DSS	Water	3% DSS
MR120	3% DSS	Water	3% DSS	Water	3% DSS

Day 8 – Pharmacological treatments

as U/g of dry weight tissue.

2.5. Flow cytometry assays

2.5.1. Isolation of splenocytes

After suppression, the spleen was removed, mechanically dispersed through a 100 μm cell-strainer, and washed with PBS containing 0.6 mM EDTA (PBS-EDTA). The cellular suspension was then centrifuged at 1500 RCF for 10 min at 4 °C, the pellet re-suspended in PBS-EDTA, incubated with 2 mL of NH_4Cl lysis buffer (0.15 M NH_4Cl, 1 mM $KHCO_3$, 0.1 mM EDTA in distilled water) for 5 min, in the dark, to provoke erythrocytes lysis and centrifuged at 1500 RCF for 10 min at 4 °C. Then, pellets were washed with PBS-EDTA and re-suspended in 5 mL cell staining buffer (PBS containing 0.5% fetal calf serum (FCS) and 0.1% sodium azide). Finally, the cellular suspension was stained with fluorescent antibodies (Kruisbeek, 2001).

2.5.2. Isolation of mesenteric lymph nodes (MLN)

After suppression, harvesting of the whole MLN chain located in the mesentery of proximal colon was performed. The explanted tissue was rinsed with PBS, vascular and adipose tissues were removed to isolate MLN, mechanically dispersed through a 100 μm cell-strainer and washed with Hank's Balanced Salt Solution (HBSS) containing 5% FCS. The obtained suspension was centrifuged at 1500 RCF for 10 min at 4 °C, the pellet was washed with HBSS containing 5% FCS and re-suspended in 3 mL cell staining buffer. Finally, the cellular suspension was stained with fluorescent antibodies.

2.5.3. Immunofluorescent staining

Prior to staining with antibodies, 200 μL of cellular suspension was incubated with IgG1-Fc (1 μg/10^6 cells) for 10 min in the dark at 4 °C to block non-specific binding sites for antibodies. The following antibodies were used for fluorescent staining: Phycoerythrin-Cyanine 5 (PE-Cy5) conjugated anti-mouse CD3ε (0.25 μg/10^6 cells, catalog number 15-0031, lot number B226301), Fluorescein Isothiocyanate (FITC) anti-mouse CD4 (0.25 μg/10^6 cells, catalog number 100406, lot number B210488), PE anti-mouse CD8a (0.25 μg/10^6 cells, catalog number 100708, lot number B190687). Cells were incubated with antibodies for 1 h in the dark at 4 °C, washed with PBS to remove excessive antibody and suspended in cell staining buffer to perform flow cytometry analysis. The viability of the cellular suspension was determined through propidium iodide (PI) staining, a membrane impermeable fluorescent dye, excluded by viable cells, that emits red fluorescence by binding to DNA, thus resulting as a suitable marker for dead cells. Cells were incubated with PI 10 μg/mL for 1 min in the dark, at room temperature, and immediately subjected to flow cytometry analysis. Only PI^{-ve} cells were included in the analysis.

Samples were analyzed using InCyte™ software (Merck Millipore, Darmstadt, Germany). Cell populations were defined as follows: lymphocytes gated in the Forward Scatter (FSC)-Side Scatter (SSC) plot (FSC low: SSC low); T lymphocytes ($CD3^+$ lymphocytes); $CD4^+$ T lymphocytes ($CD3^+CD4^+CD8^-$ lymphocytes); $CD8^+$ T lymphocytes ($CD3^+CD8^+CD4^-$ lymphocytes). Percentages of $CD4^+$ T lymphocytes and $CD8^+$ T lymphocytes with respect to $CD3^+$ lymphocytes and the ratio between $CD4^+$ T and $CD8^+$ T lymphocytes were calculated.

2.6. Colonic cytokines levels

Colonic IL-1β, CCL20 and IL-6 levels were determined using a commercially available ELISA kits (IL-1β Mouse ELISA kit, Cusabio Technology; Mouse MIP-3α ELISA kit, Wuhan Fine Biotech; RayBio Mouse IL-6 ELISA kit, RayBiotech) in samples collected from S mice (n = 5) and DSS-treated animals administered with vehicle (n = 5) or MR120 1 mg/kg (n = 5) at the end of the protocol treatment. After being weighed, each specimen was homogenized in ice-cold 0.02 M sodium phosphate buffer (pH 4.7), containing 0.015 M Na_2EDTA and 1% Halt Protease Inhibitor Cocktail (ThermoFisher Scientific), and subjected to 3 cycles of freezing and thawing. After centrifugation for 5 min at 5000 RCF at 4 °C, the supernatant was analyzed in accordance to the manufacturers' protocols and the total protein concentration was quantified using Pierce BCA protein assay kit (ThermoFisher Scientific).

Colonic concentrations of cytokines were determined in duplicate in 100 μL samples: the absorbance was measured spectrophotometrically at 450 nm (TECAN Sunrise™ powered by Magellan™ data analysis software, Mannedorf, Switzerland). The assays sensitivity was 7.8 pg/mL for IL-1β, 4.7 pg/ml for CCL20 and 2 pg/ml for IL-6. Results were expressed as ng/g protein.

2.7. Colonic histology and immunohistochemistry (IHC)

Colonic samples were harvested from S mice (n = 5) and DSS-treated animals administered with vehicle (control group, n = 5) or MR120 1 mg/kg (n = 5) and immersion-fixed in 10% neutral buffered formalin overnight. Following standard methods, 3-5 mm-annular samples were embedded in paraffin tissue blocks, from each of which at least five transverse 3-5 μm-thick histological sections were obtained. Sections were stained by hematoxylin-eosin for a general assessment of histological damage; in case of IHC analysis, sections were blocked, incubated with rabbit primary antibody against CCR6 (bs-1542R) (1:200), followed by conjugation to the secondary antibody, staining by 3, 3′-diaminobenzidine (DAB) and counterstained with Harris hematoxylin.

Both the inflammatory infiltrate intensity and the CCR6 positivity were semi-quantitatively assessed by an unaware observer. The large bowel inflammatory infiltrate was evaluated on a 0-to-4 grade scale: 0, absent; 1, mild infiltrate (involvement of less than 25% of the wall); 2, moderate infiltrate (between 25% and 50%); 3, moderate-to-severe infiltrate (between 50% and 75%); 4, severe infiltrate (between 75% and 100%). The CCR6 IHC positivity was quantified as follows: 0, absent; 1, mild (less than 25% positive cells); 2, moderate positivity (between 25% and 50% positive cells); 3, moderate-to-high positivity (between 50% and 75% positive cells); 4, very high positivity (between 75% and 100% positive cells). The average values of histological score and of $CCR6^+$ cells recruitment were determined for each colon, pooled with those determined for the colons of the other animals in the same experimental group and the median values were calculated.

2.8. Drugs, antibodies and reagents

3-methyl-N-(4-(trifuoromethyl)phenyl)benzofuran-2-carboxamide (MR120) was synthesized and characterized by us as reported in reference (Martina et al., 2022) and was dissolved in saline solution containing DMSO 1% the day of the experiment. FITC anti-mouse CD4, PE anti-mouse CD8 and propidium iodide were purchased from BioLegend™ (San Diego, CA, USA), PE-Cy5 anti-mouse CD3 from Affymetrix eBioscience™ (San Diego, CA) and IgG1-Fc from Millipore™ (Merck, Darmstadt, Germany). TNBS, ethanol, HTAB, hydrogen peroxide, tetramethylbenzidine, dimethyl formamide and all the other reagents were purchased from Sigma Aldrich™ (St. Louis, MO, USA).

2.9. Statistics

All data were presented as mean ± SEM. Comparison among experimental groups was made using analysis of variance (one-way or two-way ANOVA) followed by Bonferroni's post-test, when $P < 0.05$, chosen as level of statistical significance, was achieved. Non-parametric Kruskal-Wallis analysis, followed by Dunn's post-test, was applied for statistical comparison of MS and cytokines levels. All analyses were performed using Prism 9 software (GraphPad Software Inc. San Diego, CA, USA).

3. Results

3.1. DSS-induced inflammatory responses

The repeated exposure to DSS produced a cyclic worsening of Control (C) mice clinical conditions, mainly due to body weight loss (data not shown), represented by the fluctuating trend of Disease Activity Index (DAI): it reached the highest values over days 9–12 and 22-25, corresponding to the wash-out periods after each DSS cycle, while, during the third phase of DSS exposure (days 30–33), DAI values were comparable to the pre-wash-out period of the first two cycles and not significantly different from S values. Interestingly, the treatment with MR120 1 mg/kg s. c., applied from day 8, progressively attenuated colitis severity in correspondence to the peaks of the DAI score, remarkably improving the clinical conditions after just a few days of treatment, and not affecting the DAI during the last DSS cycle (Fig. 2).

The assessment of the area under the curve (AUC) of the DAI-time profiles, from day 1 to day 33, confirmed the beneficial effects displayed by MR120 on murine health conditions during the entire experimental protocol (Fig. 2; up right inset). The severity of the colitis induced by the cyclic exposure to DSS was also demonstrated by the alterations revealed on day 33: macroscopic injury of the colonic mucosa (Fig. 3a), increased spleen size (Fig. 3b), augmented colonic and lung myeloperoxidase activity (Fig. 3c and d), and colonic shortening, thickening, and higher vascular permeability (Fig. 4) pointed towards the chronicization of the inflammatory responses. Repeated treatment with MR120 resulted in reduction of the macroscopic score, primarily due to a lower rate of erythemas (data not shown) (Fig. 3a), diminished spleen enlargement (Fig. 3b), and lowered myeloperoxidase activity, suggestive of decreased activation of polymorphonuclear leukocytes, especially in intestinal tissues (Fig. 3c). Although the shortening and thickening of the colon induced by cyclic DSS was not modified (Fig. 4a and b), the increased vascular permeability was significantly mitigated in the MR group (Fig. 4c).

3.2. Flow cytometry assays

Regarding the changes induced on adaptive immune cells in secondary lymphoid tissues, the cyclic exposure to DSS decreased the percentage of T cells both in the spleen and mesenteric lymph nodes (MLN) (Fig. 5) while no relevant modifications in $CD4^+$ and $CD8^+$ subpopulations of T lymphocytes were detected (Table 2; Fig. S1): the treatment with MR120 attenuated the splenic egress of $CD3^+$ cells but no effects were noted on MLN or on T lymphocytes subgroups (Fig. 5 and Table 2).

3.3. Evaluation of cytokine levels

The phlogistic state promoted by chronic DSS was demonstrated also by the remarkable increase of IL-6, dampened, although not significantly, by MR120, while the colonic levels of IL-1β and CCL20 were not modified, either by chronic DSS or by the treatment with MR120 (Fig. 6).

3.4. Histological and immune-histological analysis

The histological analysis of murine large bowel, collected at the conclusion of the experimental protocol (day 33), showed that the DSS cyclic administration produced a condition of pronounced colonic inflammation, characterized by marked epithelial hyperplasia, diffuse infiltration of inflammatory cells both in the mucosa and submucosa (Fig. 7c), and the recruitment of $CCR6^+$ elements (Fig. 7d) with respect to sham mice (Fig. 7a and b). On the basis of the morphological properties, the enrolled $CCR6^+$ cells were recognized as represented almost exclusively by lymphoid cells. Recruitment of $CCR6^+$ neutrophils was sporadic and not relevant. The treatment with MR120 did not attenuate the morphological alterations and lymphoid recruitment detected in the colonic wall (Fig. 7e and f) and scored in Fig. 8a and b.

4. Discussion

Increased interest in the CCL20/CCR6 axis in the pathogenesis of IBD, and of other autoimmune-mediated inflammatory diseases depending on the same axis, prompted us to obtain deeper insights regarding the anti-inflammatory efficacy of our recently synthesized CCR6 antagonist MR120. This compound is the very first example of a small-molecule modulator of the CCL20/CCR6 axis able to improve health conditions and to prevent colon and systemic neutrophil recruitment in an acute murine model of colitis, thus representing a promising starting point to develop an alternative therapeutic approach for IBD patients.

It is by now well-known that CCL20 is overexpressed in inflammatory conditions by a variety of immune and non-immune cells (Lee et al., 2013) and attracts CCR6-expressing leukocytes, represented mainly by antigen-presenting cells, T and B lymphocytes, and activated neutrophils, towards the phlogistic sites (Kulkarni et al., 2017). In particular, the CCL20/CCR6 pathway apparently contributes to the amplification of intestinal inflammation, as evidenced by clinical and preclinical data, such as the plasmatic and intestinal augmented levels of both CCL20 and CCR6 in IBD patients (Skovdahl et al. 2015, 2018), and the lower severity of murine experimental colitis when the axis was interrupted in CCR6-knockout mice (Varona et al., 2003) or following the administration of anti-CCL20 neutralizing antibodies (Katchar et al., 2007; Teramoto et al., 2005).

On these grounds, we designed, synthesized, and tested in *in vitro* and *in vivo* assays MR120, a small-molecule targeting the CCR6 receptor, demonstrating its promising anti-chemotactic actions and its anti-inflammatory activity against murine TNBS-induced colitis and

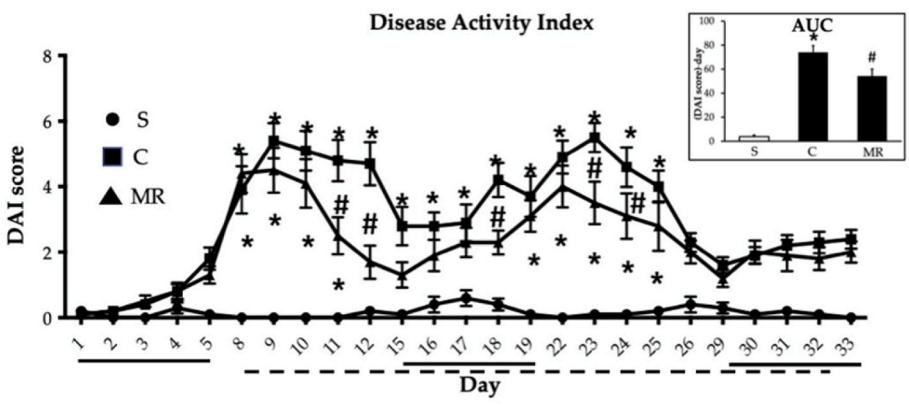

Fig. 2. Curves representing the disease activity index score, assessed during DSS-induced chronic colitis from day 1 to day 33, in vehicle-treated normal mice (● S) and colitic mice administered with vehicle (■ C) or MR120 1 mg/kg (▲ MR). Horizontal continuous lines on the bottom indicate DSS exposure, the dashed lines indicate the application of the subcutaneous pharmacological treatments. In the inset, histogram representing the area under DAI curves (AUC), from day 1 to day 33, and assessed in vehicle-treated normal mice (S) and colitic mice administered with vehicle (C) or MR120 1 mg/kg (MR) (n = 9–11 independent values per group). *P < 0.05 vs. S mice; #P < 0.05 vs. C mice; two-way or one-way (AUC) ANOVA followed by Bonferroni's post-test.

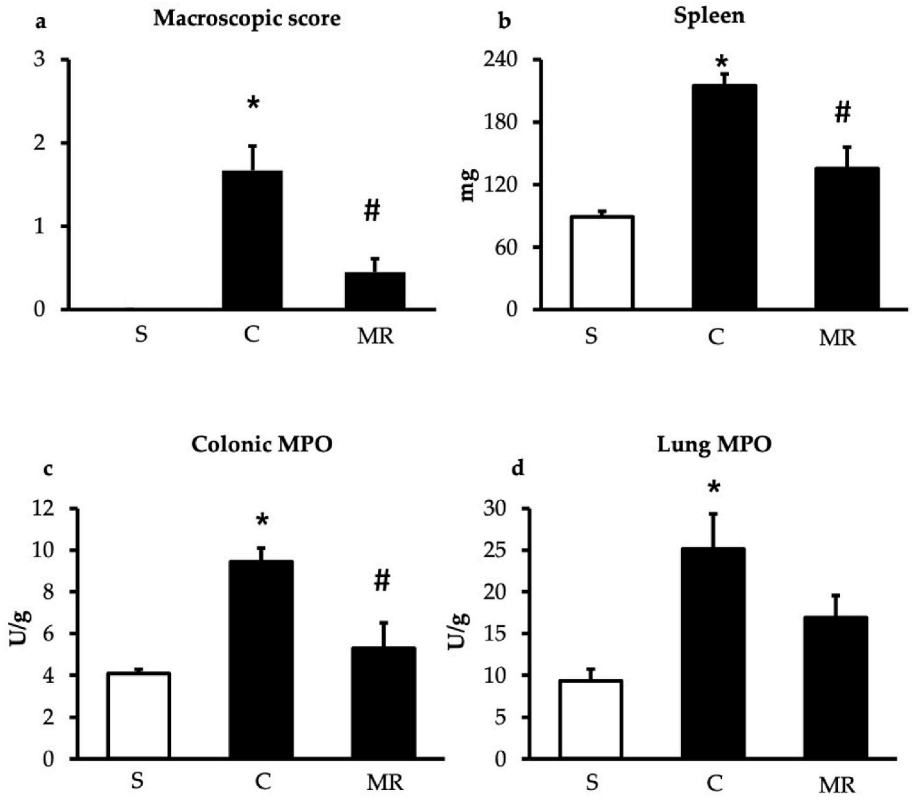

Fig. 3. Effects of MR120 on cyclic DSS-induced inflammatory responses. Macroscopic score (**a**), spleen weight (**b**), colonic (**c**) and lung (**d**) MPO activity, assessed in vehicle-treated normal mice (S) and colitic mice administered with vehicle (C) or MR120 1 mg/kg (MR) (n = 9–11 independent values per group). *P < 0.05 vs. S mice; #P < 0.05 vs. C mice; one-way ANOVA followed by Bonferroni's post-test; Kruskal-Wallis followed by Dunn's post-test (for macroscopic score).

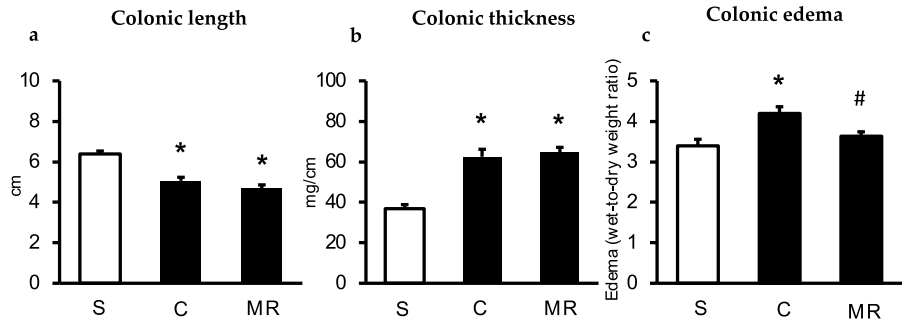

Fig. 4. Effects of MR120 on colonic length (**a**), thickness (**b**) and edema (**c**) assessed in vehicle-treated normal mice (S) and colitic mice administered with vehicle (C) or MR120 1 mg/kg (MR) (n = 9–11 independent values per group). *P < 0.05 vs. S mice; #P < 0.05 vs. C mice; one-way ANOVA followed by Bonferroni's post-test.

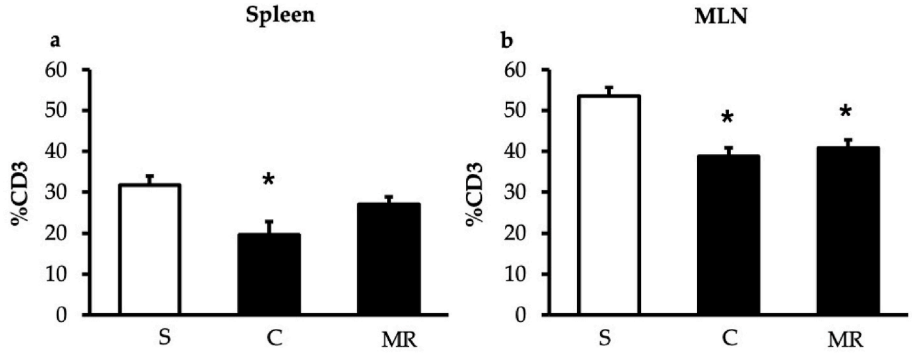

Fig. 5. Splenic (**a**) and MLN (**b**) T lymphocytes in vehicle-treated normal mice (S) and DSS-treated mice administered with vehicle (C) or MR120 1 mg/kg (MR) (n = 6–8 independent values per group). Results are expressed as %CD3$^+$ on total lymphocytes. *P < 0.05 vs. S mice, one-way ANOVA followed by Bonferroni's post-test.

Table 2
Effects of MR120 on spleen and MLN T cells count.

Treatment	SPLEEN			MLN		
	%CD4$^+$	%CD8$^+$	CD4/CD8	%CD4$^+$	%CD8$^+$	CD4/CD8
S	54.1 ± 1.2	38.1 ± 1.5	1.4 ± 0.1	54.4 ± 1.3	39.1 ± 1.2	1.4 ± 0.1
C	50.6 ± 1.7	41.3 ± 2.0	1.3 ± 0.1	52.5 ± 1.3	38.8 ± 1.7	1.4 ± 0.1
MR	52.3 ± 2.0	40.1 ± 1.7	1.3 ± 0.1	49.7 ± 1.3	43.2 ± 1.1	1.2 ± 0.1

Percentages of CD4$^+$ and CD8$^+$ T lymphocytes, and the ratio between CD4$^+$ and CD8$^+$ T cells were assessed in the spleen and MLN excised from vehicle-treated normal mice (S) and DSS-treated mice administered with vehicle (C) or MR120 1 mg/kg (MR).

zymosan-induced peritonitis (compound **1b** in (Martina et al., 2022)). In order to verify whether MR120 was able to maintain its protection against a long-lasting condition of intestinal inflammation, we tested its potential anti-inflammatory action in sub-chronic DSS-induced colitis, a well-established model of recurrent intestinal inflammation characterized by face validity (ability to replicate the human disease phenotype) and predictive validity (similarity in pharmacological responsiveness between the animal model and the human condition) (Valatas et al., 2015).

In our investigation, the three-cycle drinking of DSS for 33 days produced a periodical trend of increase and decline of colitis severity, corresponding to the alternating phases of relapse and remission of clinical symptoms and mimicking the typical, recurring tidal stream of IBD responses (Bento et al., 2012). In particular, a striking worsening of murine health conditions was observed during the wash-out periods after each cycle of DSS, as expected on the basis of the literature, while milder body changes were registered in the final part of the protocol, during the recovery phase. Indeed, repeated exposure to two-cycle drinking of DSS over three weeks is considered sufficient to promote a stable, chronic colitis, endowed with predictive validity (Bento et al., 2012; Bylund-Fellenius et al., 1994). It should also be remembered that, when considering a model of colitis developed to mimic a pathological condition characterized by alternating peaks and troughs, the value of DAI assessed in days during one of the phases of recovery cannot precisely mirror the concurrent level of some of the inflammatory responses in specific body regions, perhaps better represented by the area under the curve of DAI profile over time. Likewise, the increase of some typical markers of inflammation, such as inflammatory cytokines, could follow a different time profile and result not markedly modified at day 33. Yet, various local and systemic inflammatory responses had increased by the end of the experimentation, while DAI values in colitic mice were not significantly different from those of sham mice. Regarding colonic alterations, mucosal and submucosal injuries and morphological changes of the intestinal wall were detected, along with the increased production of IL-6, described as a mediator of intestinal and extra-intestinal IBD manifestations (Neurath, 2014). Remarkable to note was the recruitment of CCR6$^+$ cells, histologically recognized as lymphoid cells, an effect confirming the lymphocytes accumulation in colonic micro-vessels already documented by (Teramoto et al., 2005), and the oxidative action of neutrophils in the colon and lungs, expressed by increased myeloperoxidase activity and representative of the involvement of the innate immune system. Finally, it is worth mentioning that the cyclic exposure to DSS elicited splenomegaly, a typical phenomenon already documented by (Axelsson et al., 1998) as a consequence of repeated exposure to the colitogenic agent and expression of the increased spleen workload, although not necessarily related to higher leukocytes cellularity (Wang et al., 2013). Interestingly, spleen enlargement is a feature that has also been noticed in ulcerative colitis and Crohn's disease patients and has been strongly correlated with IBD severity (Kawashima et al., 2022).

Treatment with MR120 was able to attenuate colitis severity by controlling, with different efficacy, some of the systemic and local inflammatory responses. The daily administration of the small molecule significantly improved overall mice conditions, as demonstrated by the notable reduction of the area under DAI curve. Regarding the effects of MR120 at the colonic level, histological injury, colonic shortening and thickening, and intestinal infiltration of CCR6$^+$ lymphoid cells, presumably consequences of the outflow of T lymphocytes from MLNs to

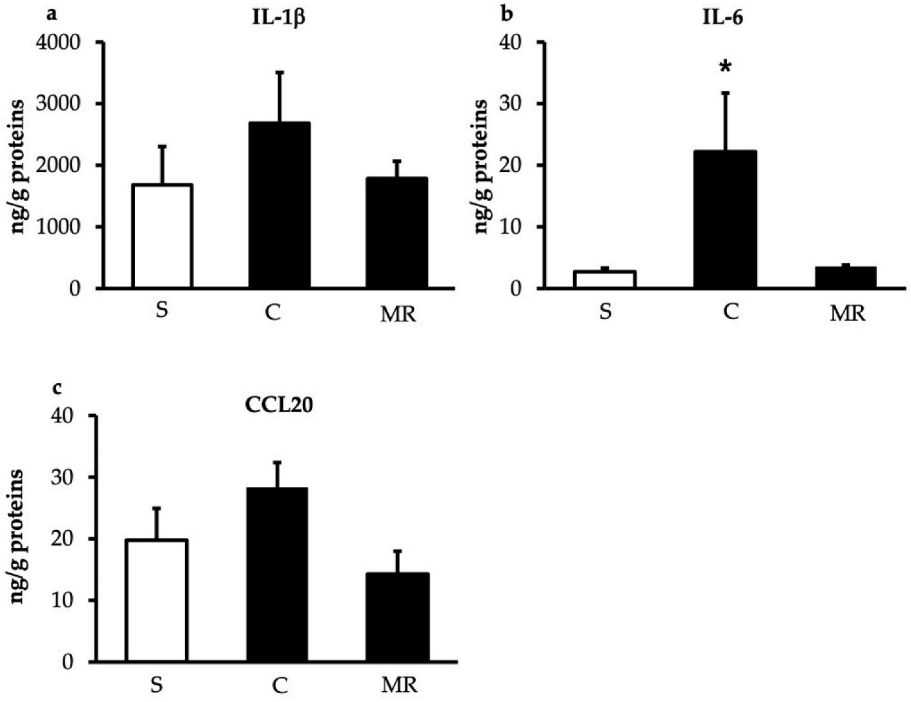

Fig. 6. IL-1β (**a**), IL-6 (**b**) and CCL20 (**c**) levels in colonic tissues excised from vehicle-treated normal mice (S) and DSS-treated mice administered with vehicle (C) or MR120 1 mg/kg (MR) (n = 3–6 independent values per group). *P < 0.05 vs. S mice, one-way ANOVA followed by Bonferroni's post-test.

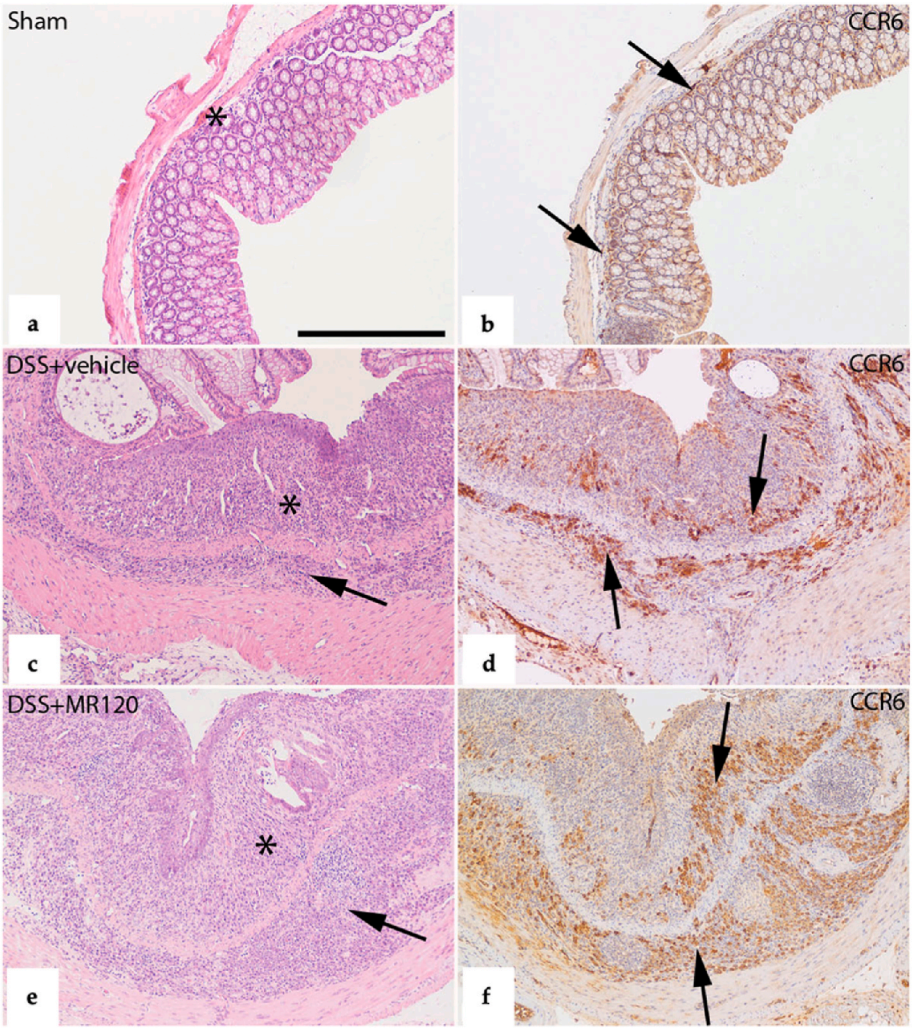

Fig. 7. Representative histological sections, stained by hematoxylin-eosin (**a**, **c** and **e**), and immunehistochemical sections, labeled with anti-CCR6 antibody and stained by 3,3′-diaminobenzidine (DAB) (**b**, **d** and **f**), of colonic specimens harvested from vehicle-treated S mice (**a**, **b**) and from chronic DSS-treated mice administered with vehicle (**c**, **d**) or MR120 1 mg/kg (**e**, **f**). In panels **a**, **c** and **e**, infiltration of inflammatory cells is highlighted both in the mucosa (asterisks) and in the submucosa (arrows). In panels **b**, **d** and **f**, the infiltration of CCR6^{+} lymphoid elements is marked by arrows. Scale bar: 400 μm.

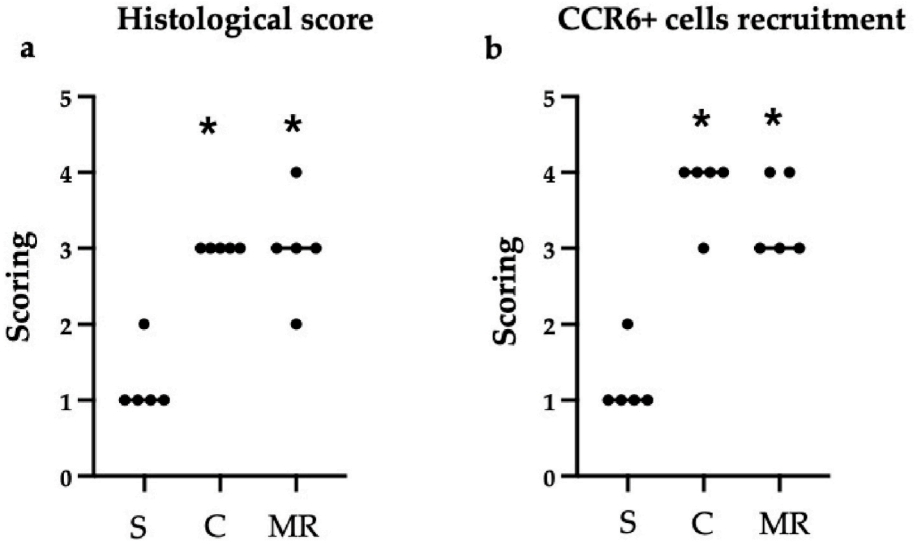

Fig. 8. Scoring of histological damage (**a**) and of CCR6^{+} cells infiltration (**b**) of colonic specimens harvested from vehicle-treated S mice and from chronic DSS-treated mice administered with vehicle (C) or MR120 1 mg/kg (MR). Horizontal bar is at the median value. *$p < 0.05$ vs. S mice, Kruskal-Wallis followed by Dunn's post-test.

the gut *lamina propria*, were not prevented at the very end of the colitis protocol. Nonetheless, MR120 lowered the mucosal macroscopic score and slightly attenuated the gut levels of IL-6 (Neurath, 2014), probably contributing, through a cascade effect, to decrease the colonic edema and the oxidative activity of intestinal neutrophils, suggesting an encouragingly persistent anti-inflammatory action. Finally, the novel drug counteracted also the splenomegaly and mitigated the splenic egress of T lymphocytes: the ability of MR120 to limit such a movement probably contributes to its positive effects in chronic colitis and points towards its potential interference with the CCL20/CCR6 axis.

On the basis of the collected evidence, we can draw two significant conclusions. First, the ability of MR120 to weaken, although with different efficacy, both the systemic and local inflammatory responses triggered by a continuous state of colitis are consistent with the anti-phlogistic properties already exhibited by the small molecule in two complementary models of acute gut inflammation, elicited by the stimulation of innate and adaptive immune responses (Martina et al., 2022). Second, in comparison with previous investigations, where the interference with the CCL20/CCR6 axis was obtained through the application of anti-CCL20 neutralizing monoclonal antibodies and mainly local effects emerged (Katchar et al., 2007; Teramoto et al., 2005), our data emphasize the efficacy of the small molecule MR120 not only in dampening bowel changes but also in improving murine general health conditions. As regards to the mechanism of the anti-inflammatory action of MR120, *in vitro* functional studies have demonstrated the ability of the small molecule to interfere with the CCL20-induced recruitment of immune cells (Martina et al., 2022): this activity possibly underlies the acceleration of the process of recovery and shut-down of inflammation, detectable at a macroscopic level rather that in the histological and immune-histochemical detail of the colonic mucosa. Although MR120 presented a suboptimal *in vitro* potency (Martina et al., 2022) and unclear modulation of some inflammatory parameters that characterize the sub-chronic *in vivo* model under study, this molecule is the first-known modulator of the CCL20/CCR6 axis showing efficacy in well recognized IBD *in vivo* models and deserves further study to develop more potent derivatives as possible candidates for IBD and other autoimmune-mediated inflammatory diseases.

CRediT authorship contribution statement

Marika Allodi: Formal analysis, Investigation. **Carmine Giorgio:** Investigation. **Matteo Incerti:** Investigation. **Domenico Corradi:** Investigation. **Lisa Flammini:** Investigation. **Vigilio Ballabeni:** Writing – review & editing. **Elisabetta Barocelli:** Writing – review & editing. **Marco Radi:** Conceptualization, Formal analysis, Writing – original draft, Writing – review & editing, Funding acquisition. **Simona Bertoni:** Conceptualization, Formal analysis, Writing – original draft, Writing – review & editing, Funding acquisition, All authors have read and agreed to the published version of the manuscript.

Data availability

Data will be made available on request.

Acknowledgment

This work was supported by the University of Parma and by the European Crohn's and Colitis Organisation (to S.B. and M.R.). M.R. is member of the COST Action CA 18133 "European Research Network on Signal Transduction—ERNEST". Dr. Giuseppe Domenichini is also acknowledged for his skillful technical assistance.

Appendix A. Supplementary data

Supplementary data to this article can be found online at https://doi.org/10.1016/j.ejphar.2023.175613.

References

Alex, P., Zachos, N.C., Nguyen, T., Gonzales, L., Chen, T.-E., Conklin, L.S., Centola, M., Li, X., 2009. Distinct cytokine patterns identified from multiplex profiles of murine DSS and TNBS-induced colitis. Inflamm. Bowel Dis. 15, 341–352. https://doi.org/10.1002/ibd.20753.

Axelsson, L.G., Landström, E., Bylund-Fellenius, A.C., 1998. Experimental colitis induced by dextran sulphate sodium in mice: beneficial effects of sulphasalazine and olsalazine. Aliment. Pharmacol. Ther. 12, 925–934. https://doi.org/10.1046/j.1365-2036.1998.00357.x.

Bento, A.F., Leite, D.F.P., Marcon, R., Claudino, R.F., Dutra, R.C., Cola, M., Martini, A.C., Calixto, J.B., 2012. Evaluation of chemical mediators and cellular response during acute and chronic gut inflammatory response induced by dextran sodium sulfate in mice. Biochem. Pharmacol. 84, 1459–1469. https://doi.org/10.1016/j.bcp.2012.09.007.

Bylund-Fellenius, A.C., Landström, E., Axelsson, L.G., Midtvedt, T., 1994. Experimental colitis induced by dextran sulphate in normal and germfree mice. Microb. Ecol. Health Dis. 7, 207–215. https://doi.org/10.3109/08910609409141356.

Cooper, H.S., Murthy, S.N., Shah, R.S., Sedergran, D.J., 1993. Clinicopathologic study of dextran sulfate sodium experimental murine colitis. Lab. Invest. 69, 238–249.

Giorgio, C., Allodi, M., Palese, S., Grandi, A., Tognolini, M., Castelli, R., Lodola, A., Flammini, L., Cantoni, A.M., Barocelli, E., Bertoni, S., 2021. UniPR1331: small eph/ephrin antagonist beneficial in intestinal inflammation by interfering with type-B signaling. Pharmaceuticals 14, 502. https://doi.org/10.3390/ph14060502.

Grandi, A., Zini, I., Flammini, L., Cantoni, A.M., Vivo, V., Ballabeni, V., Barocelli, E., Bertoni, S., 2017. α7 nicotinic agonist AR-r17779 protects mice against 2,4,6-trinitrobenzene sulfonic acid-induced colitis in a spleen-dependent way. Front. Pharmacol. 8, 809. https://doi.org/10.3389/fphar.2017.00809.

Ivey, C.L., Williams, F.M., Collins, P.D., Jose, P.J., Williams, T.J., 1995. Neutrophil chemoattractants generated in two phases during reperfusion of ischemic myocardium in the rabbit. Evidence for a role for C5a and interleukin-8. J. Clin. Invest. 95, 2720–2728. https://doi.org/10.1172/JCI117974.

Kaser, A., Ludwiczek, O., Holzmann, S., Moschen, A.R., Weiss, G., Enrich, B., Graziadei, I., Dunzendorfer, S., Wiedermann, C.J., Mürzl, E., Grasl, E., Jasarevic, Z., Romani, N., Offner, F.A., Tilg, H., 2004. Increased expression of CCL20 in human inflammatory bowel disease. J. Clin. Immunol. 24, 74–85. https://doi.org/10.1023/B:JOCI.0000018066.46279.6b.

Katchar, K., Kelly, C.P., Keates, S., O'brien, M.J., Keates, A.C., 2007. MIP-3alpha neutralizing monoclonal antibody protects against TNBS-induced colonic injury and inflammation in mice. Am. J. Physiol. Gastrointest. Liver Physiol. 292, G1263–G1271. https://doi.org/10.1152/ajpgi.00409.2006.

Kawashima, K., Onizawa, M., Fujiwara, T., Gunji, N., Imamura, H., Katakura, K., Ohira, H., 2022. Evaluation of the relationship between the spleen volume and the disease activity in ulcerative colitis and Crohn disease. Medicine (Baltim.) 101, e28515. https://doi.org/10.1097/MD.0000000000028515.

Kulkarni, N., Pathak, M., Lal, G., 2017. Role of chemokine receptors and intestinal epithelial cells in the mucosal inflammation and tolerance. J. Leukoc. Biol. 101, 377–394. https://doi.org/10.1189/jlb.1RU0716-327R.

Kruisbeek, A.M., 2001. Isolation of mouse mononuclear cells. Curr. Protoc. Im. https://doi.org/10.1002/0471142735.im0301s39 (Chapter 3), Unit 3.1.

Lee, A.Y.S., Eri, R., Lyons, A.B., Grimm, M.C., Korner, H., 2013. CC chemokine ligand 20 and its cognate receptor CCR6 in mucosal T cell immunology and inflammatory bowel disease: odd couple or Axis of evil? Front. Immunol. 4, 194. https://doi.org/10.3389/fimmu.2013.00194.

Martina, M.G., Giorgio, C., Allodi, M., Palese, S., Barocelli, E., Ballabeni, V., Szpakowska, M., Chevigné, A., Piet van Hamburg, J., Davelaar, N., Lubberts, E., Bertoni, S., Radi, M., 2022. Discovery of small-molecules targeting the CCL20/CCR6 axis as first-in-class inhibitors for inflammatory bowel diseases. Eur. J. Med. Chem. 243, 114703 https://doi.org/10.1016/j.ejmech.2022.114703.

Meitei, H.T., Jadhav, N., Lal, G., 2021. CCR6-CCL20 axis as a therapeutic target for autoimmune diseases. Autoimmun. Rev. 20, 102846 https://doi.org/10.1016/j.autrev.2021.102846.

Moore-Olufemi, S.D., Kozar, R.A., Moore, F.A., Sato, N., Hassoun, H.T., Cox, C.S., Kone, B.C., 2005. Ischemic preconditioning protects against gut dysfunction and mucosal injury after ischemia/reperfusion injury. Shock 23, 258–263.

Neurath, M.F., 2014. Cytokines in inflammatory bowel disease. Nat. Rev. Immunol. 14, 329–342. https://doi.org/10.1038/nri3661.

Scheerens, H., Hessel, E., de Waal-Malefyt, R., Leach, M.W., Rennick, D., 2001. Characterization of chemokines and chemokine receptors in two murine models of inflammatory bowel disease: IL-10-/- mice and Rag-2-/- mice reconstituted with CD4+CD45RBhigh T cells. Eur. J. Immunol. 31, 1465–1474. https://doi.org/10.1002/1521-4141(200105)31:5<1465::AID-IMMU1465>3.0.CO;2-E.

Skovdahl, H.K., Granlund, A. van B., Østvik, A.E., Bruland, T., Bakke, I., Torp, S.H., Damås, J.K., Sandvik, A.K., 2015. Expression of CCL20 and its corresponding receptor CCR6 is enhanced in active inflammatory bowel disease, and TLR3 mediates CCL20 expression in colonic epithelial cells. PLoS One 10, e0141710. https://doi.org/10.1371/journal.pone.0141710.

Skovdahl, H.K., Damås, J.K., Granlund, A. van B., Østvik, A.E., Doseth, B., Bruland, T., Mollnes, T.E., Sandvik, A.K., 2018. C-C motif ligand 20 (CCL20) and C-C motif chemokine receptor 6 (CCR6) in human peripheral blood mononuclear cells: dysregulated in ulcerative colitis and a potential role for CCL20 in IL-1β release. Int. J. Mol. Sci. 19, 3257. https://doi.org/10.3390/ijms19103257.

Teramoto, K., Miura, S., Tsuzuki, Y., Hokari, R., Watanabe, C., Inamura, T., Ogawa, T., Hosoe, N., Nagata, H., Ishii, H., Hibi, T., 2005. Increased lymphocyte trafficking to colonic microvessels is dependent on MAdCAM-1 and C-C chemokine mLARC/

CCL20 in DSS-induced mice colitis. Clin. Exp. Immunol. 139, 421–428. https://doi.org/10.1111/j.1365-2249.2004.02716.x.

Trivedi, P.J., Adams, D.H., 2018. Chemokines and chemokine receptors as therapeutic targets in inflammatory bowel disease; pitfalls and promise. J Crohns Colitis 12, S641–S652. https://doi.org/10.1093/ecco-jcc/jjx145.

Valatas, V., Bamias, G., Kolios, G., 2015. Experimental colitis models: insights into the pathogenesis of inflammatory bowel disease and translational issues. Eur. J. Pharmacol. 759, 253–264. https://doi.org/10.1016/j.ejphar.2015.03.017.

Varona, R., Cadenas, V., Flores, J., Martínez-A, C., Márquez, G., 2003. CCR6 has a non-redundant role in the development of inflammatory bowel disease. Eur. J. Immunol. 33, 2937–2946. https://doi.org/10.1002/eji.200324347.

Vincetti, P., Brianza, A., Scalacci, N., Costantino, G., Castagnolo, D., Radi, M., 2016. A microwave-assisted multicomponent protocol for the synthesis of benzofuran-2-carboxamides. Tetrahedron Lett. 57, 1464–1467. https://doi.org/10.1016/j.tetlet.2016.02.068.

Wang, Y., Han, G., Chen, Y., Wang, K., Liu, G., Wang, R., Xiao, H., Li, X., Hou, C., Shen, B., Guo, R., Li, Y., Chen, G., 2013. Protective role of tumor necrosis factor (TNF) receptors in chronic intestinal inflammation: TNFR1 ablation boosts systemic inflammatory response. Lab. Invest. 93, 1024–1035. https://doi.org/10.1038/labinvest.2013.89.